35th International Electric Vehicle Symposium and Exhibition (EVS35)
Oslo, Norway, June 11-15, 2022

CFD parametric optimisation of a Direct Liquid Cooling based prototype for HEV/EV

M. Larrañaga-Ezeiza[1,2], G. Vertiz[1], I. Galarza[1], P.F. Arroiabe[2], M. Martinez-Agirre[2], J. Berasategi[2]

[1] *CIDETEC, Basque Research and Technology Alliance (BRTA), Po. Miramón 196, 20014 Donostia-San Sebastián, Spain (mlarranaga@cidetec.es)*

[2]*Mechanical and Industrial Production Department, Faculty of Engineering, Mondragon Unibersitatea, Loramendi 4, E-20500 Arrasate-Mondragón, Spain*

Summary

In this work, a numerical optimisation process is proposed to improve the fluid dynamical aspect of an innovative direct liquid cooling strategy for lithium-ion based HEV/EV. Using the CFD numerical environment, the battery cell simulation model was characterised and validated with experimental information. Then, a comparison between different flow patterns was developed to analyse the influence of the fluid distribution geometry. Finally, a parametric multi-objective optimisation process was implemented to obtain the optimal relationship between the thermal performance of the battery cell, the volumetric energy density of the system, and the power consumption of the strategy.

Keywords: Lithium battery, Thermal management, Finite element calculation, Cooling, Energy density, Research

1 Introduction

Aiming to reduce CO_2 emissions in densely populated areas, in recent years HEV/EV vehicles have been one of the global benchmark topics in the mobility sector [1]. Considering batteries as the energy source, these technologies enable 100% zero-emission operation. Nowadays, due to the characteristic large density, high discharge capacity and low maintenance, Li-ion based batteries are the reference technology in the electric vehicle sector.

Although this energy storage technology has high electrical performance, the proper operation of these types of systems is influenced by the temperature at which they operate. The thermal management of these systems is therefore essential. To avoid premature degradation of the energy storage system and prevent risky situations, the optimal working range of lithium-ion batteries is between 15-40 ℃ [2][3], maintaining a cell level temperature uniformity of 0-5 ℃. These temperature ranges ensure the best compromise between technical performance and system safety [4].

To control the working temperature of the battery system, in recent years different cooling strategies have been considered. These strategies are generally classified as air cooling, Liquid Cooling (LC), Phase Change Materials (PCM), Heat Pipes (HP), and Thermoelectric coolers (TEC) [5]. Among these technologies, owing to the thermal conductivity and heat capacity of the implemented fluids, strategies based on Liquid Cooling (LC) predominates the thermal management of the electric vehicle sector [6]. LC strategies can be divided into two main groups, Indirect Liquid Cooling (ILC) and Direct Liquid Cooling (DLC). Nowadays, ILC is the leading strategy in the field of electric vehicles. However, the fluids used in ILC are electrically conductive, nature that avoids direct contact with the battery cell. This characteristic decreases the cooling capacity of the strategy compromising the performance of the system [7][8]. Consequently, DLC has been the subject of many studies in recent years [9][10][11][12][13]. DLC strategy uses dielectric fluids with high dielectric strength that enable direct contact between the heat generation source (battery cell) and the refrigeration fluid, consequently improveing the thermal management efficiency of the system [14].

Recently, some studies have been carried out to analyse the features that can be improved in DLC strategy to achieve optimal system performance. These types of optimisation processes are developed in the numerical environment using Multiphysics models to characterise the real working conditions of the system. An example of this type of analysis is the study that Y. Fan et al. [15] developed with a battery module based on 32 cylindrical cells with a direct liquid cooling strategy. Using as a reference a full immersed casuistry, the authors analysed the effect of partial cooling by reducing the height of the fluid channel. Results presented that the thermal behaviour of the battery module was worsened by decreasing the height of the fluid channel. However, the authors highlighted that the power consumption of the auxiliary system and the energy density of the battery module improved because of the lower pressure drop and weight. Considering other design parameters, in the development process of a novel direct liquid immersion cooling strategy, M.-Y. Lee et al. [16] analysed the effect of the cell spacing on the system performance. Using as a reference a battery module of 14 pouch type cells of 20Ah, the study results presented that cell temperatures and pressure drop of the system improve increasing cell spicing. However, the authors mentioned that in a practical scenario, the lowest cell spicing is preferred due to the use of space in the battery system. Finally, X. Ju et al. [17] performed a geometrical optimisation analysis using a manifold immersion cooling structure for a 51 Ah prismatic battery module. Defining a uniform heat generation on the battery, the structure of the manifold was parametrised to analyse the influence of the fluid line geometry on the thermal and fluid dynamical performance of the strategy. As a result, at expense of a minor pressure drop increase, a higher and more homogeneous heat transfer coefficient was led on the surface of the battery cells decreasing maximum temperatures and thermal heterogeneities of the system.

Based on the above literature review, it is appreciated the importance of analyse the influence of the design parameters to improve the performance of the cooling strategy and thus, develop a robust, effective, and economical design. Therefore, in this article, a design optimisation of a direct liquid cooling prototype is proposed. However, instead of analysing the influence of the parameters independently, this work proposes an optimization process based on the design of experiments methodology (DoE) to analyse the influence of the interaction of the parameters on the fluid dynamical results, and thus, achieve more accurate results for the design optimization.

The proposed work assumes the optimisation stage of a cell level prototype before scaling up to a module level. Considering the current market trends to increase the energy density of the HEV/EV, the prototype was developed as a refrigeration strategy of a large-scale lithium-ion 60 Ah NMC pouch type cell, a type of cell with high energy to mass ratio and packaging efficiency [18]. Moreover, the strategy was designed to develop a partial direct liquid cooling to decrease the fluid weight impact on the systems energy. In this work, to improve the aspects related to the thermal performance, energy density and power consumption of the reference prototype, an optimisation process is proposed. Using the numerical CFD environment, first, the battery cell simulation model was characterised and validated with experimental information. Then, a comparison between different flow patterns was developed to analyse the influence of the fluid distribution geometry. Finally, a parametric multi-objective optimisation process was implemented to obtain the optimal relationship between the thermal performance of the battery cell, the volumetric energy density of the system, and the power consumption of the strategy.

2 Model description

The numerical model of this strategy is defined to optimize the cell level fluid dynamical characteristics of the cooling channel before the scale-up to a module level prototype. This working stage focused on the numerical environment, was defined to achieve this goal. Ansys Fluent 21R2 was used to develop the simulation models. This software enables a coupled analysis, solving the fluid and the heat transfer accounting for a non-uniform and transitory heat generation of the battery cell.

2.1 Physical model

The partial cooling concept developed in this work is a strategy that focuses on the cooling effect on the surface of the cell body, enabling a thermal management directly focused on the battery cell. To develop this strategy, a prismatization component was designed. This component enables the internal circulation of the cooling fluid creating a space between the cell contact surface and the component's internal surface. As is shown in Figure 1, this space is designed to define the thermal management of the battery cell.

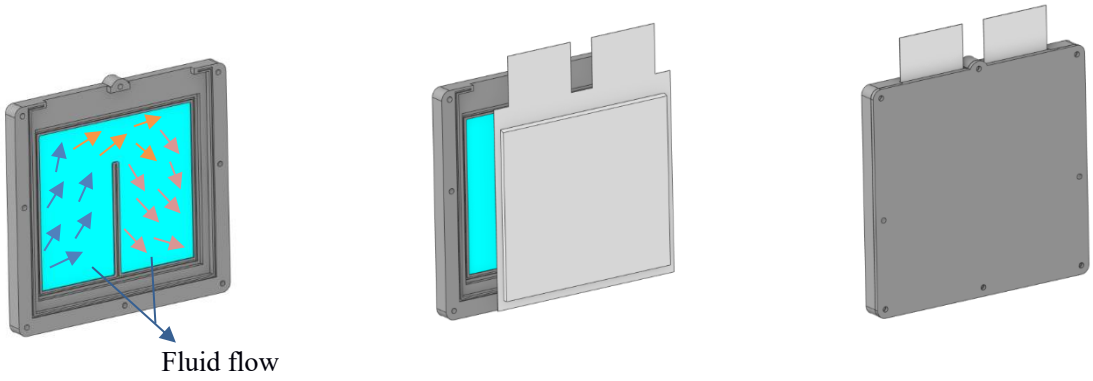

Figure 1: Reference model a) flow distribution, b) principal components, and c) assembly.

2.2 Simulation model geometry

To replicate the experimental setup, the principal components defined in the simulation model were: the battery cell, the fluid, and the clamps (Figure 2). Clamps were implemented because of the influence they have on the thermal behaviour of the battery cell. These components have almost ten times the mass impact of the battery tabs and were used to develop the electrical connexion of the tests.

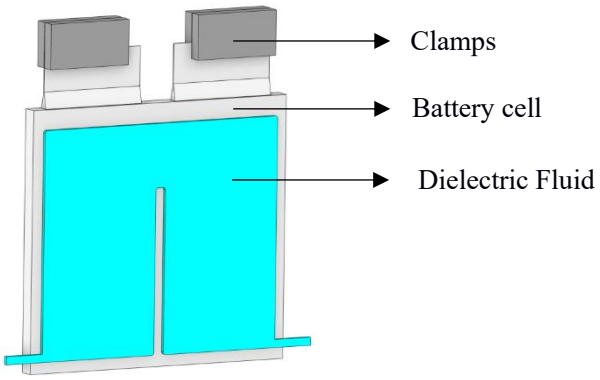

Figure 2. Principal components defined in the simulation model.

The battery cell implemented in the model is a large scale 60 Ah NMC pouch type battery cell. As the battery cell, the dielectric fluid implemented on the model mirrors the characteristics of the commercial dielectric fluid based on mineral oil that was used in the reference prototype. The thermal and electrical characteristics of each component are presented in Table 1.

Table 1: Properties of the battery cell, the clamps, and the dielectric fluid, for 25 °C.

Property	Battery cell	Clamps	Dielectric fluid
Resistivity (MΩm)	-	-	>5·106
Material	Battery cell	Aluminum	Mineral oil
Kinematic Viscosity (mm^2/s)	-	-	4.3
Heat Capacity (J/kgK)	1306.36	871	2130
Thermal conductivity (W/mK)	x,y: 17.9 / z:0.65	202.4	0.135
Density (kg/m^3)	2183.31	2719	774

2.3 Battery modelling

The heat generation of a Li-ion battery can be expressed by the simplified equation of Newman $Q_{gen}=Q_{irr}+Q_{rev}$. Where Q_{gen} is the total heat generation (W), Q_{irr} is the irreversible heat (W), and Q_{rev} is the reversible heat. The irreversible heat generation, also referred as Joule effect, is represented by equation $Q_{irr}=I^2 R_{int}$ (SOC, T). Where I is the current (A) and R_{int} the internal resistance of the cell (Ω). On the other hand, the reversible heat generation is developed by the insertion and disinsertion of lithium ions into the electrodes (the anode and the cathode). This generation is based on the electrochemical reactions that take place when discharging and charging the lithium-ion cells, reactions that create a variation in the entropic level of the system. This generation is represented by equation $Q_{rev}=IT\,dE_{OCV}/dT$. Where I is the current (A), T is the temperature (K), and dE_{OCV}/dT the variation of the open circuit voltage respect temperature (V/K).

To characterise the heat generation of the battery cell numerically, an electrothermal model was implemented to mirror the thermal response of the battery cell properly. This model calculates the heat generation of the cell considering the instantaneous temperature (T) and the State of Charge (SOC) level. Moreover, this model characterises the influence of the current density increase on the thermal behaviour of the battery cell at high C-rate working conditions.

In this aspect, to characterise the battery cell, the Equivalent Circuit Model (ECM) was selected on the battery module of Ansys Fluent 21R2, a model that is widely used because of its simplicity and effectiveness [19]. Working with experimental Hybrid Pulse Power Characterization (HPPC) testing data, the parameters of the equivalent circuit model were calculated. This characterization mirrors only the irreversible heat generation of the battery cell. Therefore, to characterize the endothermic behaviour of the battery cell, the entropic factor of the reversible heat generation was implemented by User Define Functions (UDFs). This factor was experimentally characterised analysing the Open Circuit Voltage variation in temperature (dE_{OCV}/dT).

The battery cell heat generation model was validated using experimental voltage and temperature information of a 1C discharge test (Figure 3). The simulation model was initialised at the same State of Charge (SOC) and temperature level as the experimental test. A SOC level of 100 % and a temperature of 25 ºC, consecutively. The discharge process was followed until the SOC level of 20 % was reached. To characterise the interaction between the climatic chamber and the prototype, an equivalent heat transfer coefficient of 25 W/m^2K was defined on the boundary surfaces of the battery cell [20][21], a convective value experimentally validated.

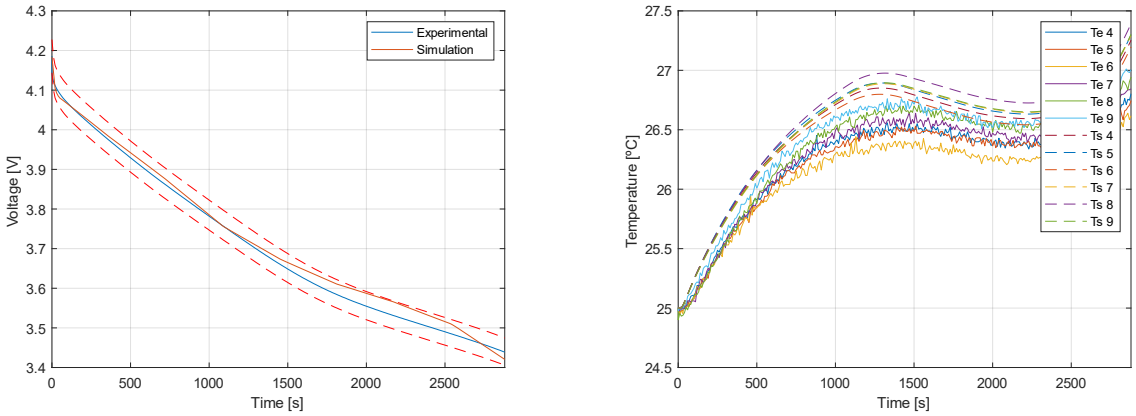

a) *b)*

Figure 3. Battery cell model validation with experimental a) voltage, and b) surface temperature distribution in a range of 100%-20% SOC

Pulse profiles in a SOC range of 40%-50% were implemented to analyse the influence of the geometrical parameters of the fluid channel on aspects related to the thermal performance, energy density and power consumption of the proposed strategy. These tests were developed until the thermal stabilization of the battery cell, thus, dynamics effects during the tests were avoided to analyse more clearly the influence of the parameters under study. Therefore, the heat generation of the battery cell model in charging and discharging process was analysed between a SOC range of 80 % - 20 %, SOC range where the charging process and the discharging process have a similar heat generation. As presented in Figure 4, results of the simulation model reflect at the same magnitude the heat generation range of the battery cell and the shape that represents it.

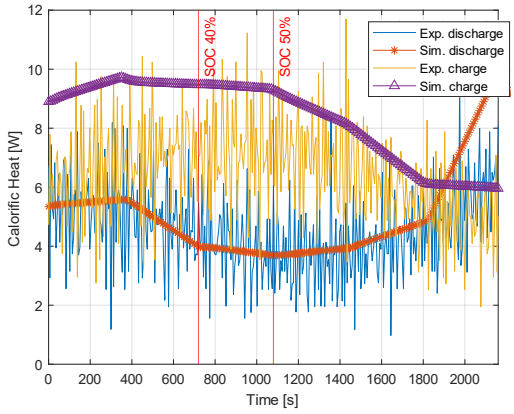

Figure 4. Battery cell model heat generation validation with experimental heat generation information 100%-20% SOC range.

2.4 Mesh independence

To define proper mesh for accurate results, a mesh independence study was developed using as a reference the particular case of the U-Shape flow pattern design analysed on the geometrical comparison section (Section 3). To analyse the stabilization of the maximum temperature of the battery cell and the pressure drop of the cooling strategy, sensitivity study was developed using seven models with different grid cell numbers. All cases were analysed defining constant inlet fluid flow and temperature at 0.4 l/min and 25 ºC, consecutively. The defined flow rate of 0.4 l/min is calculated using the characteristics of an indirect liquid cooling strategy based coldplate as a reference [22]. The laminar model was defined to characterise the flow development due to the Reylonds

number being lower than 2300 in all case studies. To characterise the cell heat generation, a 1C pulse profile was implemented. Owing the prototype prismatization casing, the interaction of the cell body with the climatic chamber environment was omitted. Therefore, an adiabatic definition was imposed on the battery cell surface that was not in contact with the fluid. On the tab zone and on clamps an equivalent heat transfer coefficient of 25 W/m^2K was defined. As Figure 5 presents, maximum temperature and pressure drop curves are stabilised with a mesh of 4778025 elements. Where the results variation maintains below 1% when the elements where increased to 8743816. Thus, it was concluded that the results are independent from mesh for the model with 4778025 elements [23][24].

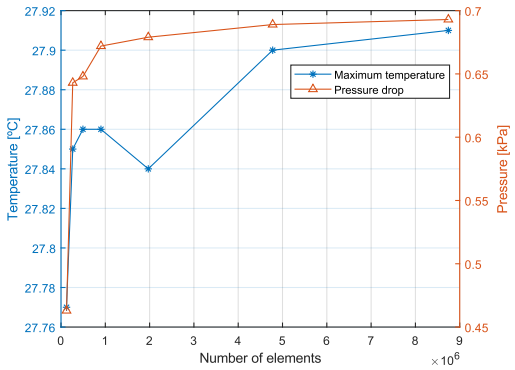

Figure 5. Mesh independence analysis about the maximum temperature of the battery cell (ºC) and pressure drop (kPa).

3 Flow pattern design selection

Before optimizing the geometrical aspect of the prototype flow pattern, a design selection process was specified. This process was aimed at selecting among different flow pattern geometries analysed in the bibliography [23]. Defining the same working conditions, a comparison between the four main designs presented in Figure 6 was developed: U-Shape, Convex, Honeycomb and Airfoil. The objective of this study was to analyse the impact that the geometry of the pattern had on the flow rate distribution, and the resultant thermal performance and power consumption of each of the prototype.

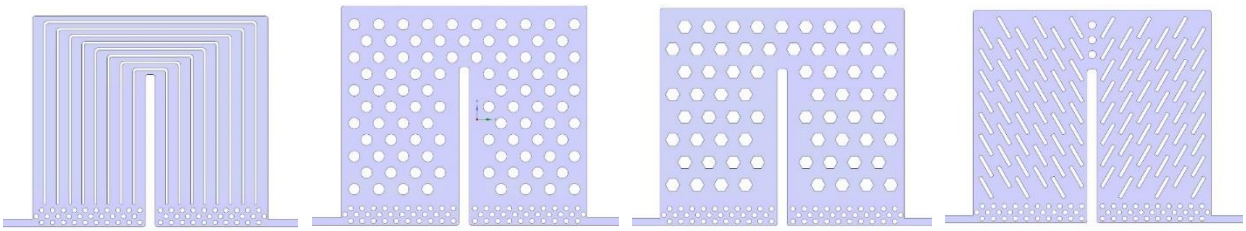

a) b) c) d)

Figure 6: Flow pattern designs a) U-Shape, b) Convex, c) Honeycomb and d) Airfoil

To make the designs comparable, same surface contact areas between the battery cell and flow patterns were defined at 0.026 m^2, a conditioning parameter to define same heat absorption capacity with same fluid volume in all flow pattern designs.

3.1 Boundary conditions

As a variable of the study, simulations at a flow rate of 0.1, 0.2, 0.4, 0.8, and 1.6 l/min were developed with each flow pattern design. This study of the working range makes it possible to draw the curves for each case and thus,

to develop the comparison between the flow rate designs in a wide working range. The inlet temperature of the fluid and the boundary temperature that mirrors the climatic chamber influence were defined at 25 ºC. As previously mentioned, an adiabatic definition was imposed on the battery cell surface that was not in contact with the fluid. On the tab zone and clamps an equivalent heat transfer coefficient of 25 W/m^{2}K was defined. The battery cell working condition was defined with a 1C pulse test. These tests were developed until the thermal stabilization of the battery cell, thus, dynamics effects during the tests were avoided to analyse more clearly the influence of the parameters under study.

3.2 Results and discussion

To analyse how the flow pattern geometry influences the performance of the battery cell and the auxiliary system, battery cell maximum temperature (T_{max}), temperature homogeneity (ΔT) and the pumping power consumption related to the auxiliary system (P_h) were defined as the output variables. Figure 7 presents the steady state results of each case at flow rates of 0.1, 0.2, 0.4, 0.8, and 1.6 l/min.

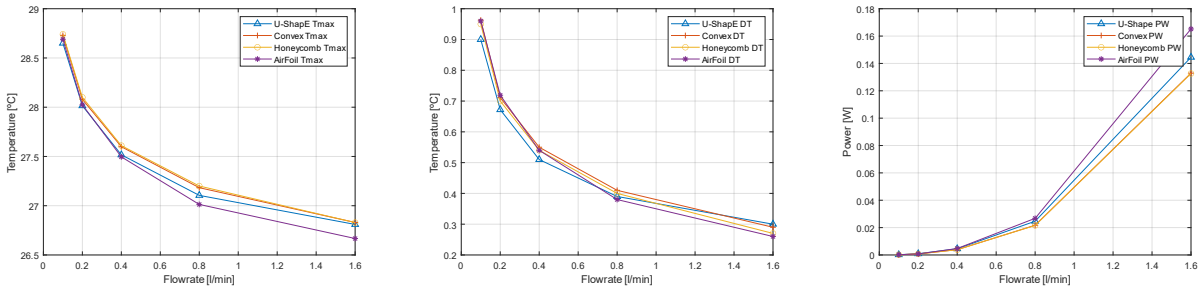

a) b) c)

Figure 7. Geometry comparison results of a) battery cell maximum temperature (T_{max}), b) temperature homogeneity (ΔT), and c) the pumping power consumption related to the auxiliary system (P_h) at different flow rate.

As it is depicted in Figure 7a and b, at high flow rates, AirFoil design is the one with the lowest battery cell temperature and homogeneity. However, at low flow rates U-Shape model presents the best thermal performance. Although the flow rate is greatly reduced, due to the channels of the U-Shape design, the flow is forced to develop all over the surface of the cell avoiding the appearance of hot spots and provides better homogeneity. Considering the power consumption impact presented in Figure 7c, Convex and Honeycomb models are the ones with the lowest pressure drop impact because the pattern design enables a higher freedom to the flow than the other design. However, this freedom hinders the flow control and facilitates the development of hot spots. This reasons why those two models have the highest maximum temperature and heterogeneity values.

To provide a more visual interpretation of the effect of each design, Figure 8 shows the surface contact temperature between the fluid and the battery cell at a flow rate of 0.4 l/min. As it is presented, U-Shape model provides the most homogenous temperature distribution in the battery cell surface.

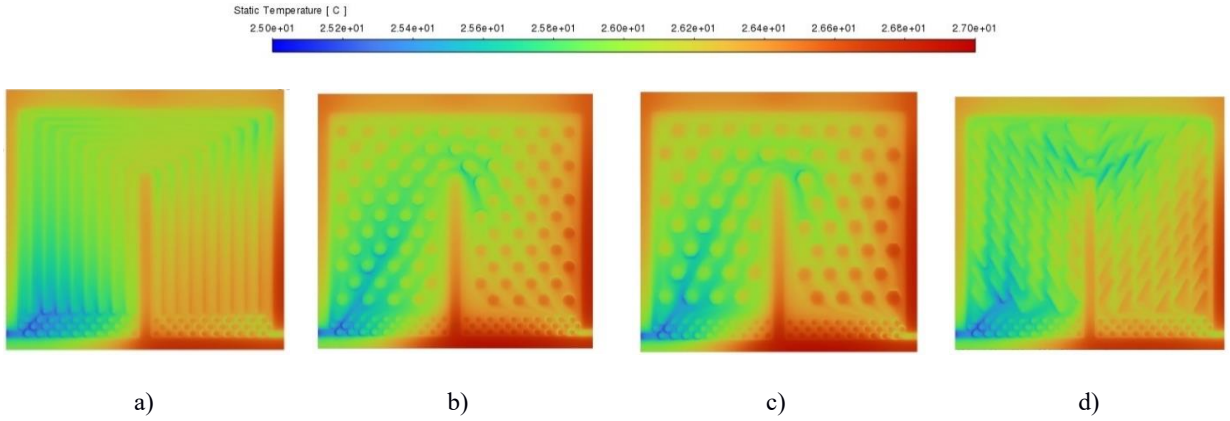

a) b) c) d)

Figure 8. Battery cell surface temperature distribution at 0.4 l/min of flow rate for a) U-Shape, b) Convex, c) Honeycomb, and d) Airfoil designs.

Considering that the prototype is defined to work with low flow rates to decrease the impact of the cooling strategy on the power consumption impact of the auxiliary system. It is concluded that the U-Shape design is the most appropriate one to develop the geometrical optimisation process that will define the reference cell level design to develop a battery module based on the direct liquid cooling strategy presented in this paper.

4 Design optimisation

4.1 Parametrisation of the geometry

To develop the multi-objective optimisation of the selected U-Shape flow pattern, four parameters were selected including the height of the fluid (H_f), the number of cooling channels (N_c), the number of inlet and outlet distributors (N_d), and the flow rate (Q). Figure 9 presents each parameter definition.

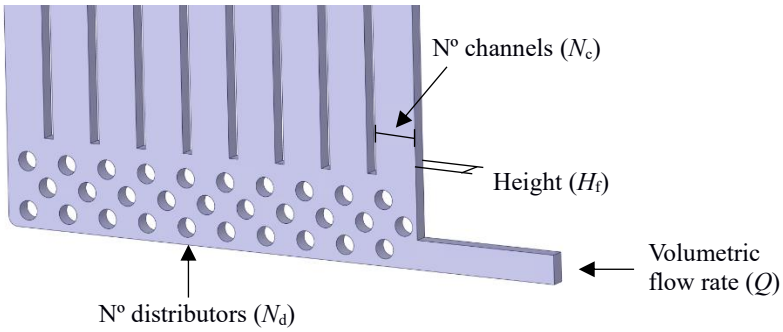

Figure 9. Parameters implemented in the optimisation process

The height of the fluid was defined from 1mm to 3mm to analyse the impact that the fluid volume reduction has on the energy density and the power consumption of the system in contrast with the effect in the thermal performance of the battery cell. The number of cooling channels and distributors were defined from 3 to 9 channels, and from 10 to 30 distributors to analyse the influence of those components to spread the fluid in a homogeneous way from all the cooling space. This definition was based on the cell surface temperature analysis presented in Figure 10. For each case the cooling channels and the distributors were omitted, and the temperature of the cell surface analysed. Considering Figure 8, it is observed that the lack of these components creates a heterogeneous fluid distribution developing hot spot areas on the battery cell surface. Finally, inlet flow rate was

defined as variable of study to analyse how impacts this input the relationship between the thermal performance of the battery system and the power consumption of the auxiliary system.

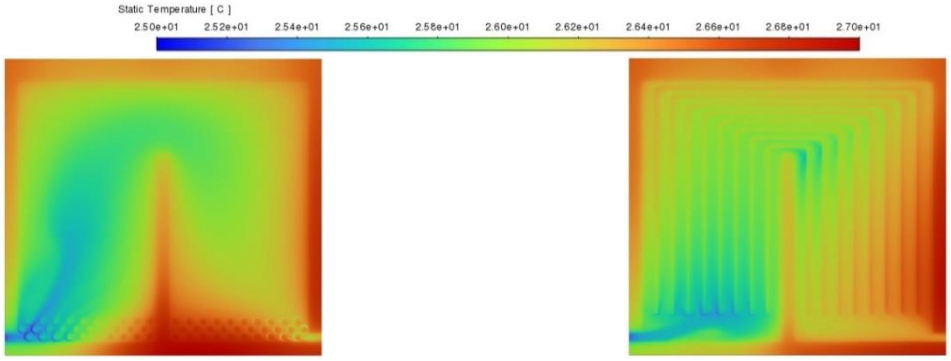

a) b)

Figure 10. Battery cell surface temperature distribution for a) a cooling design without channels and b) a cooling design without distributors

4.2 Output variables

To evaluate the performance of each case, four objective output variables were defined, including maximum temperature (T_{max}), temperature homogeneity (ΔT), system volumetric energy density (VED), and system power consumption (P_h). As it is presented in Figure 11, first two variables (T_{max} and ΔT) were related to the cell level design to analyse how the strategy controls the thermal behaviour of the battery system. Then, scaling up to a battery module of 24 battery cells, the impact of each cooling strategy on the system volumetric energy density (VED) and system power consumption (P_h) were analysed.

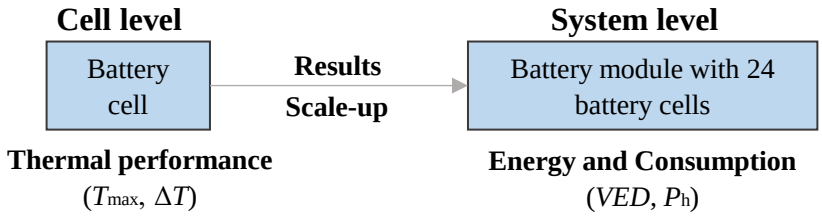

Figure 11. Output variable analysis level explanation

4.3 Optimisation process definition

To evaluate how the flow rate definition and the geometrical parameters influence the performance of the strategy, a two-level full factorial matrix was defined, an numerical analysis method that considers all the possible variations between the factors that were defined to analyse. Hence, considering four variables of study, a simulation process with 2^4 simulation cases was defined. With the proposed analysis, all the interactions between H_f, N_c, N_d, and Q were calculated. To analyse the importance of the defined variables on the output results of the full factorial design, Analysis of Variance (ANOVA) was employed, a statical model that evaluates the importance of the defined factors by comparing the response variable means at the defined factor levels. To properly develop the regression equations, all variations up to the second order of interaction between the defined factors were first analysed. Then, the most relevant interactions were selected by definen a significance level of 0.05. Once the most influential factors conditioning the output variable were selected, the factorial design was analysed again, and the ANOVA results were extracted. With this information, the regression coefficients were calculated, and

regression equations were developed for each output variable. To analyse the reliability of these regression model, values of R^2 (Adequate), R^2 (Predicted), and R^2 (Adjusted) were analysed, and the residual normal plots were presented. After the validation, the optimum case was selected considering the composite desirability function. Function where the optimum case selection process guideline was defined assigning specific weight and importance values for each of the proposed output variables.

4.4 Results and analysis

The corresponding results of the two-level full factorial design are presented in Table 2. Among the results, cell level T_{max} and ΔT, and module level *VED* and P_h output variable results can be observed for all the possible variations between H_f, N_c, N_d and Q.

Table 2: The corresponding simulation cases of the two-level full factorial design and the output variable results of each case.

Nº simulations	H_f (mm)	N_c	N_d	Q (l/min)	Cell level		Module level	
					T_{max} (ºC)	ΔT (ºC)	*VED* (Wh/l)	P_h (W)
1	3	9	30	0.4	27.52	0.51	248.70	0.1089
2	1	9	30	0.4	27	0.37	279.78	1.455
3	3	3	30	0.4	27.51	0.56	248.70	0.0948
4	1	3	30	0.4	26.98	0.38	279.78	1.301
5	3	9	10	0.4	27.56	0.47	248.70	0.0764
6	1	9	10	0.4	27.02	0.35	279.78	1.162
7	3	3	10	0.4	27.51	0.49	248.70	0.069
8	1	3	10	0.4	26.98	0.36	279.78	1.06
9	3	9	30	0.13	28.36	0.78	248.70	0.0086
10	1	9	30	0.13	27.73	0.68	279.78	0.131
11	3	3	30	0.13	28.31	0.84	248.70	0.0073
12	1	3	30	0.13	27.7	0.71	279.78	0.118
13	3	9	10	0.13	28.37	0.73	248.70	0.0065
14	1	9	10	0.13	27.72	0.65	279.78	0.115
15	3	3	10	0.13	28.27	0.76	248.70	0.0056
16	1	3	10	0.13	27.69	0.67	279.78	0.1035

To obtain the coefficients of the regression model, ANOVA was used. As it is mentioned in the optimisation procedure section, these coefficients were evaluated using the most relevant interactions effects between the defined factors. Therefore, the coefficients defined for the regression equations were the ones that presents a significance level below 0.05. Considering this guideline, the following regression equations were obtained for the output variables of cell maximum temperature (T_{max}), cell surface temperature homogeneity (ΔT), system volumetric energy density (*VED*), and system power consumption (P_h):

$$T_{max} = 27.6 + 0.28H_f - 0.38\,Q \quad (1)$$

$$\Delta T = 0.58 + 0.06H_f - 0.014N_c + 0.022N_d - 0.146\,Q + 0.008H_f\,N_d + 0.01H_f\,Q \quad (2)$$

$$VED = 264.24 - 15.54H_f \quad (3)$$

$$P_h = 0.364 - 0.316H_f + 0.039N_d + 0.302\,Q - 0.031\,H_f\,N_d - 0.261H_f\,Q + 0.035N_d\,Q \quad (4)$$

To analyse the reliability of the regression model, values of R^2 (Adequate), R^2 (Predicted), and R^2 (Adjusted) were analysed, significance index that presents the adequate quality, the quality of the predicted regression models and the quality of the models after adjustment. Considering results from Table 3, index values agree for T_{max}, ΔT, *VED*. Index values for *VED* were 100 % in all R^2 cases. This result means that there is not variability on results. The volumetric energy density *VED* is the only one proportional to a single parameter (H_f). Result in agreement with the calculation of the volumetric energy density. Therefore, the quality and the correlation of these values demonstrates the reliability of the regression models.

Table 3. Values of R^2 (Adequate), R^2 (Predicted), and R^2 (Adjusted) for the output variables T_{max}, ΔT, *VED*, and P_h.

	R^2 (Adequate)	R^2 (Predicted)	R^2 (Adjusted)
T_{max}	90.32%	85.34%	88.84%
ΔT	99.68%	99.00%	99.47%
VED	100 %	100 %	100 %
P_h	99.59%	98.37%	99.23%.

Apart from R^2 index values, it is important to make sure that the results of the residuals for each response are consistent. Figure 12 presents the residual normal plots for each output variable. As it is shown the residuals are normally distributed, which means that there is a good agreement between the predicted and actual values. Figure 12c corroborates the interpretation made with R^2 index values for the volumetric energy density *VED*. Therefore, it was confirmed that *VED* was uniquely and exclusively proportional to H_f. These results demonstrated that the proposed regression models could predict adequately the variability of the output parameters. The reliability of the regression models is therefore justified.

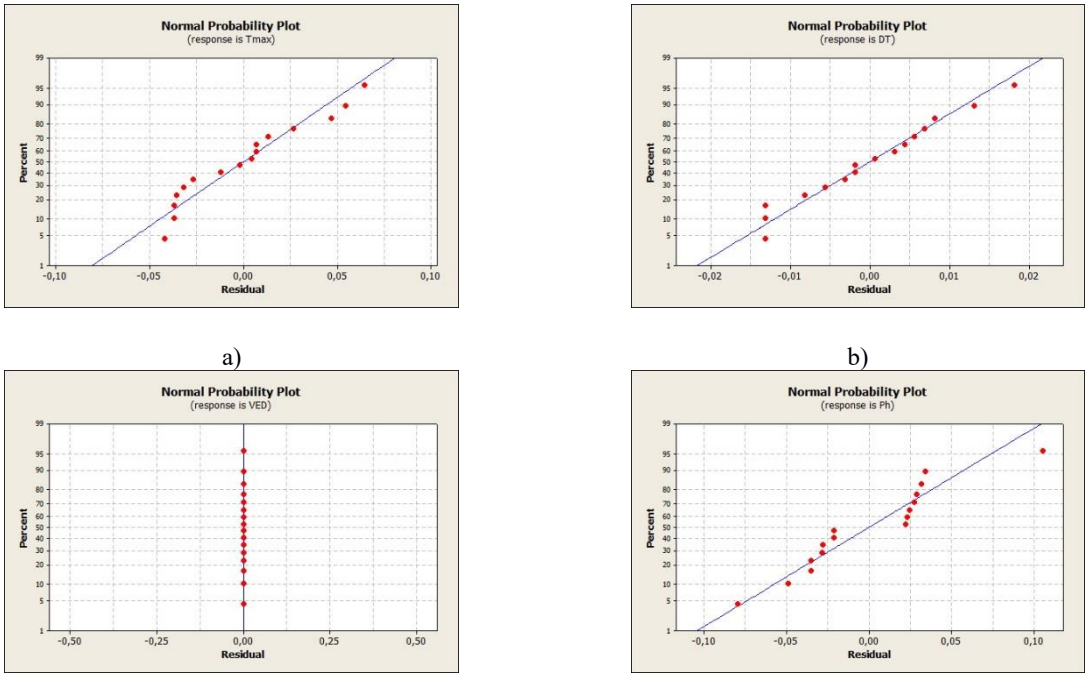

Figure 12. Residual normal plots for the output variables of a) T_{max}, b) ΔT, c) *VED*, and d) P_h.

After validating the regression models, the principal influences of the optimisation parameters on the defined output variables were analysed. As it is presented in the regression equation of cell maximum temperature (T_{max}), the height of the fluid channel (H_f), and the inlet flow rate definitions (Q) were the main parameters that influences the maximum temperature of the cell body. This means that the influence of the number of channels (N_c) and distributors (N_d) is negligible for the output variable T_{max}. However, the influence of those input parameters is appreciated on the variability of the temperature homogeneity of the battery cell surface (ΔT). With a higher N_c number, the temperature difference of the cell surface increases. Opposite influence of N_d parameter number. The results therefore recommended to decrease the number of distributors and increase the number of channels to improve the temperature homogeneity of the battery cell surface.

As mentioned above, the volumetric density (*VED*) is influenced only by the parameter H_f. Therefore, analysing the results, the objective of developing systems with high volumetric energy density will be achieved by reducing

this parameter H_f as much as possible. In this case, the minimum value of 1mm for H_f is the one that gives the best results of volumetric density.

Finally, to achieve the objective of decreasing the power consumption of the system, the regression equation presents that mainly all the parameters had an influence on it. However, analysing the estimated coefficients for P_h, it is observed that H_f, Q and the interaction between them ($H_f \cdot Q$) have more impact than the N_d, and related interactions. The power consumption of the system is based on the pressure drop defined by the fluid, therefore, H_f and Q influence is coherent. The pressure drop is related in a quadratic way by the velocity of the fluid [25]. Therefore, to decrease the power consumption of the system lower fluid velocity profiles were recommended. Analysing the influence of the parameters N_c and N_d, it can be observed that the increase in the number of channels and distributors increases the power consumption of the system. Therefore, it is concluded that the quantity of these components has to be the minimum quantity for achieveing the desired fluid distribution for the system to maintain the lowest impact on the power consumption of the system.

Once the reliability of the regression models was validated, and the principal influences of the optimisation parameters on the defined output variables were analysed, the composite desirability function for T_{max}, ΔT, VED, and P_h was implemented. This function calculates, according to the desirability values defined for each output variable, the optimal case within the range of the proposed two-level full factorial model results.

To analyse results that ensure the best performance of the battery cell, first, a composite desirability function was developed with the maximum desirability values defined for T_{max} and ΔT to minimize the temperature results. In this case, the optimum values to ensure the best thermal performance were H_f = 1mm, N_c = 9, N_d = 10, and Q = 0.4 l/min. This configuration maintains the highest volumetric energy density at expense of a considerable increase in the P output parameter. Therefore, VED and P_h were implemented with a lower weight impact and the same importance on the composite desirability function to develop a multi-objective optimisation that minimises the power consumption of the strategy and maximises the volumetric energy density of the system. For this case, the corresponding values of the design variables were H_f = 1mm, N_c = 9, N_d = 10, and Q = 0.13 l/min. Maintaining the maximum volumetric energy density of 279,7 Wh/l, this configuration imply an increase of the maximum temperature from 27,02 ºC to 27,72ºC, and the temperature difference was increased by 0.3 ºC. However, the power consumption of the system was decreased by 90% from 1.16 W to 0.11 W.

5 Conclusions

In this work, a parametric optimisation of a direct liquid cooling strategy is proposed for a large-scale lithium-ion pouch type cell as a reference. First, the simulation model was developed and validated with experimental results. A non-uniform heat generation was defined in the battery model to adequately represent the temperature distribution of the large-scale pouch type cell. Then, a comparison between different flow pattern designs was developed to analyse the influence of the fluid distribution geometry. Finally, a parametric optimisation process was implemented to obtain the optimal relationship between the thermal performance of the battery cell, the volumetric energy density of the system, and the power consumption of the strategy. The analysis in the present work gave rise to the following conclusions:

- At flow rates below 0.4 l/min, the flow distribution channels defined on the U-Shape design improve the fluid dynamical aspect of the cooling strategy maintaining the highest thermal performance of the battery cell without increasing the power consumption impact on the system. It was therefore selected to develop the parametrisation process.
- Developed surrogate models presented that the most critical parameters that influence the output variable results were the height of the fluid channel (H_f) and the flowrate definition (Q), which are directly related to the fluid velocity.
- The number of channels (N_c) increases the power consumption of the system (P) while decreasing the thermal heterogeneity of the battery cell (ΔT). Therefore, while the thermal distribution of the cell remains within the optimal range, it is recommended to decrease the number of channels.

- The number of distributors (N_d) increases the power consumption of the system (P) and the thermal heterogeneity of the battery cell (ΔT). However, a minimum number of components to adequately distribute the inflow and outflow are necessary, thus, avoiding hot spots in the system.
- The proposed parametric optimisation defined the optimum design of the DLC strategy that ensures the optimal relationship among T_{max}, ΔT, *VED*, and P_h. The corresponding values of the design parameters were H_f = 1mm, N_c = 9, N_d = 10, and Q = 0.13 l/min, a design case that maintains T_{max} at 27.72 and ΔT at 0.65 with the maximum *VED* value and reducing P_h by 90%.

Acknowledgments

This research did not receive any specific grant from funding agencies in the public, commercial, or not-for-profit sectors.

References

[1] International Energy Agency, "Global EV Outlook 2020," *Glob. EV Outlook 2020*, 2020, doi: 10.1787/d394399e-en.

[2] V. G. Choudhari, D. A. S. Dhoble, and T. M. Sathe, "A review on effect of heat generation and various thermal management systems for lithium ion battery used for electric vehicle," *J. Energy Storage*, vol. 32, no. March, p. 101729, 2020, doi: 10.1016/j.est.2020.101729.

[3] X. Han *et al.*, "A review on the key issues of the lithium ion battery degradation among the whole life cycle," *eTransportation*, vol. 1, p. 100005, 2019, doi: 10.1016/j.etran.2019.100005.

[4] M. S. Patil, J. H. Seo, S. Panchal, S. W. Jee, and M. Y. Lee, "Investigation on thermal performance of water-cooled Li-ion pouch cell and pack at high discharge rate with U-turn type microchannel cold plate," *Int. J. Heat Mass Transf.*, vol. 155, p. 119728, 2020, doi: 10.1016/j.ijheatmasstransfer.2020.119728.

[5] J. Kim, J. Oh, and H. Lee, "Review on battery thermal management system for electric vehicles," *Appl. Therm. Eng.*, vol. 149, no. November 2018, pp. 192–212, 2019, doi: 10.1016/j.applthermaleng.2018.12.020.

[6] C. Rouaud, "Automotive Thermal Management," 2020.

[7] Y. Chung and M. S. Kim, "Thermal analysis and pack level design of battery thermal management system with liquid cooling for electric vehicles," *Energy Convers. Manag.*, vol. 196, no. May, pp. 105–116, 2019, doi: 10.1016/j.enconman.2019.05.083.

[8] C. Yang and L. Cao, "The role of interfacial thermal resistance in Li-ion battery thermal management," *ASME 2019 Int. Tech. Conf. Exhib. Packag. Integr. Electron. Photonic Microsystems, InterPACK 2019*, no. February, 2019, doi: 10.1115/IPACK2019-6594.

[9] 3M, "3M Novec 7000 engineered fluid product information," pp. 1–6, 2005, [Online]. Available: http://multimedia.3m.com/mws/mediawebserver?66666UuZjcFSLXTtlXftMxMVEVuQEcuZgVs6EVs6E666666--.

[10] "XING Mobility Dynamic Power on Demand," 2022. https://www.xingmobility.com/assets/pdf/XingMobility_DynamicPower_OnDemand.pdf.

[11] Kreisel Battery, "Kreisel Battery Pack," 2022. https://www.kreiselelectric.com/.

[12] S. Park and D. Jung, "Battery cell arrangement and heat transfer fluid effects on the parasitic power

consumption and the cell temperature distribution in a hybrid electric vehicle," *J. Power Sources*, vol. 227, pp. 191–198, 2013, doi: 10.1016/j.jpowsour.2012.11.039.

[13] D. W. Sundin and S. Sponholtz, "Thermal Management of Li-Ion Batteries With Single-Phase Liquid Immersion Cooling," *IEEE Open J. Veh. Technol.*, vol. 1, pp. 82–92, 2020, doi: 10.1109/ojvt.2020.2972541.

[14] P. Dubey, G. Pulugundla, and A. K. Srouji, "Direct comparison of immersion and cold-plate based cooling for automotive li-ion battery modules," *Energies*, vol. 14, no. 5, 2021, doi: 10.3390/en14051259.

[15] X. Tan, P. Lyu, Y. Fan, J. Rao, and K. Ouyang, "Numerical investigation of the direct liquid cooling of a fast-charging lithium-ion battery pack in hydrofluoroether," *Appl. Therm. Eng.*, vol. 196, no. June, p. 117279, 2021, doi: 10.1016/j.applthermaleng.2021.117279.

[16] M. Suresh Patil, J. H. Seo, and M. Y. Lee, "A novel dielectric fluid immersion cooling technology for Li-ion battery thermal management," *Energy Convers. Manag.*, vol. 229, no. September 2020, p. 113715, 2021, doi: 10.1016/j.enconman.2020.113715.

[17] Q. Le, Q. Shi, Q. Liu, X. Yao, X. Ju, and C. Xu, "Numerical investigation on manifold immersion cooling scheme for lithium ion battery thermal management application," *Int. J. Heat Mass Transf.*, vol. 190, p. 122750, 2022, doi: 10.1016/j.ijheatmasstransfer.2022.122750.

[18] Battery University, "Battery University - BU-301a: Types of Battery Cells," *Battery University*, 2021. https://batteryuniversity.com/article/bu-301a-types-of-battery-cells.

[19] M. K. Tran, A. Mevawala, S. Panchal, K. Raahemifar, M. Fowler, and R. Fraser, "Effect of integrating the hysteresis component to the equivalent circuit model of Lithium-ion battery for dynamic and non-dynamic applications," *J. Energy Storage*, vol. 32, no. August, p. 101785, 2020, doi: 10.1016/j.est.2020.101785.

[20] Y. Li, M. Chen, F. Bai, W. Song, and Z. Feng, "Thermal equilibrium characteristic of large-size lithium-ion pouch battery: Resting time between charge and discharge," *Energy Procedia*, vol. 158, pp. 2623–2630, 2019, doi: 10.1016/j.egypro.2019.02.013.

[21] X. Wu, S. Lv, and J. Chen, "Determination of the optimum heat transfer coefficient and temperature rise analysis for a lithium-ion battery under the conditions of Harbin city bus driving cycles," *Energies*, vol. 10, no. 11, 2017, doi: 10.3390/en10111723.

[22] M. Larrañaga, "Design and implementation of a Direct Liquid Cooling strategy for HEV/EV focus on a pouch type cell body refrigeration," in *Thermal Management Systems Symposium (21TMSS)*, 2021.

[23] M. Li, J. Wang, Q. Guo, Y. Li, Q. Xue, and G. Qin, "Numerical Analysis of Cooling Plates with Different Structures for Electric Vehicle Battery Thermal Management Systems," *J. Energy Eng.*, vol. 146, no. 4, pp. 1–10, 2020, doi: 10.1061/(ASCE)EY.1943-7897.0000648.

[24] S. Panchal, R. Khasow, I. Dincer, M. Agelin-Chaab, R. Fraser, and M. Fowler, "Numerical modeling and experimental investigation of a prismatic battery subjected to water cooling," *Numer. Heat Transf. Part A Appl.*, vol. 71, no. 6, pp. 626–637, 2017, doi: 10.1080/10407782.2016.1277938.

[25] G. O. Brown, "The history of the Darcy-Weisbach equation for pipe flow resistance," *Proc. Environ. Water Resour. Hist.*, vol. 40650, no. January, pp. 34–43, 2002, doi: 10.1061/40650(2003)4.

Authors

Manex Larrañaga received the B.S. in Energy Engineering in 2017 and in 2019 he received the M.S. in Industrial Engineering. Both by Mondragon Unibertsitatea (MU), Basque Country, Spain. A university that offers a training and learning experience that combines the educational and research needs of companies, organisations, and society. Nowadays, he is developing the PhD Programme in Applied Engineering at CIDETEC Energy Storage. A reference research centre that works concentrates in advance knowledge generation and how to translate it into technology that can be smoothly transferred to the industry.